Chapter 8

Development of Falling Film Heat Transfer Coefficient for Industrial Chemical Processes Evaporator Design

Muhammad Wakil Shahzad,
Muhammad Burhan and Kim Choon Ng

Additional information is available at the end of the chapter

http://dx.doi.org/10.5772/intechopen.69299

Abstract

In falling film evaporators, the overall heat transfer coefficient is controlled by film thickness, velocity, liquid properties and the temperature differential across the film layer. This chapter presents the heat transfer behaviour for evaporative film boiling on horizontal tubes, but working at low pressures of 0.93–3.60 kPa as well as seawater salinity of 15,000–90,000 mg/l or ppm. Owing to a dearth of literature on film-boiling at these conditions, the chapter is motivated by the importance of evaporative film-boiling in the process industries. It is observed that in addition to the above-mentioned parameters, evaporative heat transfer of seawater is affected by the emergence of micro-bubbles within the thin film layer, particularly when the liquid saturation temperatures drop below 25°C (3.1 kPa). Such micro-bubbles are generated near to the tube wall surfaces, and they enhanced the heat transfer by two or more folds when compared with the predictions of conventional evaporative film-boiling. The appearance of micro-bubbles is attributed to the rapid increase in the specific volume of vapour, i.e. dv/dT, at low saturation temperature conditions. A new correlation is thus proposed in this chapter and it shows good agreement to the measured data with an experimental uncertainty less than ±8%.

Keywords: low pressure evaporation, falling film evaporation, horizontal tubes evaporators

1. Background

In process industries such as the refineries, food and desalination plants, the need of high-performance evaporators is paramount to minimize irreversibilities due to high heat transfer as well as to reduce footprint area of associated components. A falling film evaporator is one of

the key design components which are associated with not only high heat transfer rates but are also immune to change in feed qualities. In particular, for present desalination application, the falling film evaporative process could augment heat transfer rates involving brines which inherently reduce the equipment cost because of compact design.

In this chapter, a horizontal tube falling film evaporator is studied for low-temperature applications, particularly for the desalination industry. The first part of this chapter focuses on advantages of horizontal tube falling film evaporators over flooded evaporators and vertical tube evaporators and its applications. In the second part of the chapter, a literature review on falling film evaporation heat transfer coefficient (FFHTC) to the extent necessary for this work is provided. A novel FFHTC for low-temperature (below ambient) applications and for different salt concentrations is developed in the third part of this chapter. The comparison of proposed correlation with traditional Han and Fletcher [1] correlation and the effect of different operational parameters on heat transfer is discussed in the last section of the chapter.

Flooded evaporators have been used in desalination industry for long time. Recently, there is a thrust of horizontal tubes falling film evaporators over the flooded evaporators because of their advantages. They also replaced the vertical tube evaporators because of its unique characteristics. Falling film evaporators in general, are highly responsive to operational parameters, such as energy supply, pressure levels, feed rate, and salt concentrations in the feed. The fact that falling film evaporators can be operated across small temperature differences make them amenable to the application in multiple effect configurations. The advantages of falling film evaporators are outlined in the section below.

2. Advantages of falling film evaporators

The main advantages of falling film evaporators over flooded evaporators are as follows:

1. High heat transfer coefficient and resulting compact design.
2. More uniform overall heat transfer coefficient value across the tube bundle.
3. Reduction in working fluid requirement to about one-third as compared to flooded evaporators.
4. Short product contact times, typically just a few seconds per pass.
5. Minimization of salt deposition on tubes surface that helps in cleaning the tubes.

The potential advantages of horizontal tube evaporators over vertical tubes evaporators are as follows:

1. Heat transfer coefficients for horizontal tubes are higher than those for vertical tubes since the heated flow length is much shorter.
2. External enhancements are available for tubes in copper, copper-nickel and stainless steel, etc. for up to a 10-fold increase in evaporation coefficient.

3. A horizontal tube bundle can have multiple tube passes of the heating fluid to significantly increase its heat transfer coefficient as compared to vertical tubes evaporators with single pass.
4. A larger Length to diameter ratio (L/D) ratio horizontal shell evaporator can be designed as compared to small L/D ratio of vertical evaporator that helps to prevent the dry out and flooding in the tubes.
5. The two pass (U-tube) design in horizontal tube evaporators is much more efficient, cheaper and easier to maintain compared to the single pass floating head in vertical tubes.
6. Flow length of liquid film in a horizontal tube evaporator minimizes the liquid hold-up time and residence time during operation.
7. Horizontal tubes bundle arrangement reduces the unit height that helps to reduce the piping work.
8. Horizontal arrangement reduces the footprint for large-capacity plant because the evaporators can be arranged in double tier arrangement.

Although the horizontal tubes falling film evaporators have advantages over flooded and vertical tubes evaporators, the main limitation is the lack of heat transfer data particularly at low temperature, i.e., below 323 K.

3. Heat transfer review for falling film evaporators

A critical appreciation of the thermal performance is essential for the optimum design of falling film horizontal tube evaporators especially for desalination industry. A large number of empirical and theoretical heat transfer coefficients correlations are available in literature. The majority of those available correlations are for different refrigerants, and few of them are for pure water and limited to saturation temperatures more than 323 K.

Many researchers provided the detailed overview of available correlations. A critical review is published by Ribatski and Jacobi [2] who tabulated the heat transfer correlations in terms of dimensionless numbers as developed by many researchers. They also provided heat transfer coefficient values for water and different refrigerants with single-tube and multi-tube evaporators. They concluded that every correlation has a limited validation governed by operating parameters under which they developed, and efforts are needed to generalize these correlations. Adib et al. [3] conducted the experiment with vertical tube falling film evaporator, and they calculated the heat transfer coefficient value using correlation available in literature [4–8] and found good agreement with experimental results. Uche et al. [9] compared the heat transfer correlations at different inlet brine temperatures and for different mass velocities for horizontal and vertical tube evaporators. They also compared their results with different available correlations [1, 10–14] and found that Parken correlation can be used for nonboiling conditions, and Han and Fletcher's correlation is good for boiling conditions. A falling film evaporation analytical model is developed by Fujita et al. [15–17] using R-11, and they

analysed the drip pattern, droplets, and sheet modes. They found that accuracy of their model is within ±20%.

Table 1 summaries heat transfer correlations of many researchers found in the literature. This table also highlights the limitations of applications of these correlations, such as the types of working fluids, pressures and the temperature ranges and evaporator geometry.

Since operational and design parameters are the key factors to maximize the evaporator performance, so researches are provided extensive data on it. Film modes are controlled by film Reynolds numbers, and different heat transfer coefficient behaviours are noticed by researchers for smooth tubes as Reynolds number changes [15, 18–21]. They observed three kinds of behaviour such as (1) heat transfer coefficient decreases to its minimum value and then increases again, (2) it increases with Reynolds number, and (3) heat transfer coefficient increases to its maximum value and then drops. Lorenz and Yung [22] investigated that film evaporation on a single tube is different to an array of tubes, and it may be due to turbulence of inter-tube evaporation. They also found that critical Reynolds number affects the evaporation heat transfer, and for below 300, the heat transfer coefficient value for a single tube is higher as compared to an array of tubes. Thome et al. [23] conducted the experiments for falling film heat transfer coefficient for four types of tubes, such as plain, turbo-BII HP, Gewa-B and high-flux tubes. They concluded that for different inter-tube flow modes, there is no discernible difference in heat transfer coefficients in respective flow zone. Fujita et al. [15] investigated that the heat transfer value is low on the top row of tubes which is due to direct expose to feed supply. They also investigated the effect of feeder type on heat transfer coefficient. They used refrigerant R-11 on horizontal tube evaporators. Liu et al. [18] performed falling film heat transfer experiments for different tubes surfaces, and they concluded that the value is from 3- to 4-folds higher for roll-worked tubes as compared to smooth tubes. They also found that both the flow conditions and tubes spacing have negligible effect on the heat transfer coefficient. Aly et al. [24] conducted the tests for deposit film thickness effects, and they found drastic decrease in heat transfer with increase in deposition thickness. Moeykens et al. [25, 26] and Chang et al. [27] performed falling film experiment tests for R-123, R-134a, R-22, and R-141b, and they found that it can be enhanced by adding the collection tray under each tube row. The falling film correlations developed by researchers [26, 28–30] for refrigerants R-22, R-123, R-134a, and R-141b are having uncertainty of 20–25% by using four different apparatuses. Bourouni et al. [31] performed the experiments with aero-evaporator, and they reported that increase in characteristic dimensions of heat exchanger results in a significant increase in the evaporative performance. Yang and Shen [32] found that the heat transfer coefficient is a strong function of heat input and increases with heat input. The vapour flow effect due to liquid drag and dry out of tubes is studied by Ribatski and Jacobi [2]. The effect of dynamics of film on heat transfer is investigated by Xu et al. [33] and Yang and Shen [34]. They found that increase in liquid load causes perturbation in film that enhances the heat transfer. They also reported that increase in tube diameter does not favour heat transfer which can be due to more turbulence in film on smaller diameter tubes. For horizontal tubes falling film evaporators, Han and Fletcher [1] is the most famous correlation, whereas Chun and Seban [35] is used for vertical tube. Both of these famous correlations are for pure water and for saturation temperatures of 322 K or more.

References	Correlation
Xu et al. [33]	$h_{\text{evaporation}} = 05.169 \times 10^{-11} \left[\frac{h_{fg} \cdot g \cdot \rho_1^2 \cdot D^2}{\Delta t^2 \cdot \mu_l}\right]^{-0.333} \left(\frac{\overline{\delta}}{D}\right)^{-0.422\Delta t^{0.503}} \left(1 + \frac{\delta_{\max} - \delta_{\min}}{\overline{\delta}}\right)$
	Deionized water, 50°C, horizontal copper tubes evaporator.
Fujita et al. [15]	for 1st tube:
	$Nu = \left((\text{Re}_f)^{-2/3} + 0.008(\text{Re}_f)^{0.3}(\text{Pr})^{0.25}\right)^{1/2}$
	For 2nd to 5th tubes:
	$Nu = \left((\text{Re}_f)^{-2/3} + 0.01(\text{Re}_f)^{0.3}(\text{Pr})^{0.25}\right)^{1/2}$
	Freon R-11, electrically heated five horizontal copper tubes, OD-25 mm
Han and Fletcher [1]	$h_{\text{evaporation}} = 0.0028. \left[\frac{\mu_l^2}{g.\rho_l^2.k_l^3}\right]^{-0.333} (\text{Re}_\Gamma)^{0.5}(\text{Pr})^{0.85}$
	Pure water, 49–127°C, electrically heated single horizontal tube, OD-50.8 mm, thickness-1.7 mm, Length-254 mm
Bourouni et al. [31]	$h_f = 2.2. \left[\frac{v_f^2}{g.k_l^3}\right]^{-0.333} . \left(\frac{H}{OD}\right)^{0.1} . (\text{Re}_f)^{-0.333}$
	Pure water, 60 and 90°C, Polypropylene horizontal tubes aero-evaporator , OD-25.4 mm,

http://dx.doi.org/10.5772/intechopen.69299

References	Correlation
Chun and Seban [35]	$h_{\text{film}} = 0.821.\left[\frac{\mu_l^2}{g.\rho_l^2.k_l^3}\right]^{-0.333}(\text{Re}_\Gamma)^{-0.22}$ Pure water, 46–118°C, electrically heated single vertical tube, OD-28.58 mm, thickness-0.1 mm, Length-292 mm
Alhusseini et al. [36]	For laminar region: $h^*_{\text{laminar}} = 2.65.(\text{Re})^{-0.158}(Ka)^{0.0563}\lim_{x\to\infty}$ For combine: $h^* = (h^5_{\text{laminar}} + h^5_{\text{turbulent}})^{1/5}$ Propylene glycol and water
Shmerler et al. [37]	$h^*_{\text{E}} = 0.0038.(\text{Re}_\Gamma)^{0.35}(\text{Pr})^{0.95}$ Pure water, electrically heated single vertical tube, OD-25.40 mm, Length-781 mm
Chien et al. [38]	$Nu_{cv} = 0.0386.(\text{Re}_\Gamma)^{0.09}.(\text{Re}_\Gamma)^{0.986}$ R245fa, 5 and 20°C, horizontal smooth tubes.

Table 1. Review of heat transfer coefficient correlations for different evaporator design and operation conditions.

http://dx.doi.org/10.5772/intechopen.69299

It can be seen from the above discussion that Han and Fletcher's correlation is most frequently used for film boiling on horizontal tubes. This correlation is developed with pure water evaporating at temperatures 322 K and above. There is a lack of data for evaporative film boiling typically below ambient condition. The boiling data pertaining to saline solution of 15,000–90,000 mg/l or ppm are also scarce, and yet these conditions are particularly important for the designing of falling film evaporators for processes industries and desalination plants, such as food and beverage, multi-effect desalination (MED) and multi-stage flash evaporation (MSF). Many manufacturers, perhaps due to competition reason, are not revealing their proprietary film boiling data at these conditions. We designed experiments to develop falling film heat transfer coefficient for low-temperature evaporator typically from 279 to 300 K and pressure from 0.93 to 3.60 kPa. The new proposed correlation will be applicable for wide range of concentration evaporator design. We also presented the effect of salt concentration on heat transfer and log mean temperature difference (LMTD). The proposed designed experiments will help process industries to design falling film evaporators for wide range of operation.

4. Falling film heat transfer coefficient development

The methodology used here is to adopt Han and Fletcher's correlation for film boiling on horizontal tubes and to enhance its use by incorporating the effects of salinity and by expanding the range of temperatures of its application for horizontal tubes falling film evaporation.

4.1. Theoretical model

The non-dimensional terms in Han and Fletcher correlation model, namely, the Reynolds, Prandtl and Nusselt numbers are adequate to describe the surface evaporation from liquid film due to thermal effect. At low saturation pressures, the vapour specific volume rapidly increases, and this could possibly leads to enhancement of heat transfer. Han and Fletcher model is revisited to capture this additional heat transfer enhancement phenomenon. At a low saturation temperature the micro-bubble generated at tube surface can lift up quickly because of high specific volume and break through the thermal barrier within liquid film. The traditional heat transfer models are unable to define this augmentation of heat transfer enhancement by buoyancy fortified bubble agitation.

The Han and Fletcher correlation given in **Table 1** can also be expressed in a more familiar form as shown in Eq. 1

$$\frac{h_{\text{evap}}\left(\frac{\mu_l^2}{g\rho_l^2}\right)^{1/3}}{k_l} = Nu = 0.0028(\text{Re}_\Gamma)^{0.5}(\text{Pr})^{0.85} \tag{1}$$

where indices and the constant term are found for the boundary conditions of film boiling. For the determination of the overall heat transfer coefficient, the total heat transfer is computed via heat transferred to circulating water, i.e.

$$Q_{\text{in}} = \dot{m}_{\text{ch,w}}\, Cp_{\text{ch,w}}\, (T^{o}_{\text{ch,w}} - T^{\text{i}}_{\text{ch,w}}) \tag{2}$$

Using the concept of log mean temperature difference (LMTD) and the saturation temperature of evaporator, the overall heat transfer coefficient (U_{overall}) of the evaporator can be expressed as

$$UA_{\text{overall}} = \frac{\dot{m}_{\text{ch,w}}\, Cp_{\text{ch,w}}\, (T^{out}_{\text{ch,w}} - T^{\text{in}}_{\text{ch,w}})}{\left\{ \frac{(T^{\text{out}}_{\text{ch,w}} - T_{\text{sat}}) - (T^{\text{in}}_{\text{ch,w}} - T_{\text{sat}})}{\ln \frac{(T^{\text{out}}_{\text{ch,w}} - T_{\text{sat}})}{(T^{\text{in}}_{\text{ch,w}} - T_{\text{sat}})}} \right\}} \tag{3}$$

The local falling film heat transfer coefficient on film side (h) is deduced from the knowledge of the resistance due to chilled water flow inside the tubes which is calculated by the Dittus-Boelter correlation given in Eq. 4

$$Nu = 0.023\text{Re}^{0.25}\text{Pr}^{n} \tag{4}$$

The pipe wall resistance (stainless steel 316) is negligible due to small thickness (0.7 mm). The evaporation heat transfer coefficient is calculated by using overall heat transfer coefficient given in Eq. 5

$$\frac{1}{UA} = \left(\frac{1}{hA}\right)_{\text{tubeside}} + R_{\text{wall}} + \left(\frac{1}{hA}\right)_{\text{outside}} \tag{5}$$

The experimental program is planned for capturing the two unknown parameters in above Eq. 5.

4.2. Experimental apparatus

Adsorption desalination (AD) plant existing in air-conditioning laboratory is used to conduct the experiments. **Figures 1** and **2** show the AD plant installed in National University of Singapore (NUS) and plant operational schematic.

There are five main components of AD plant namely: (1) evaporator, (2) adsorber/desorber beds, (3) condenser, (4) conditioning facility and (5) pre-treatment facility. The evaporator shell and tubes are fabricated with stainless steel and are arranged horizontally details of which are shown in **Figure 3**.

The evaporator tubes are arranged in four rows with 12 tubes in each row. This evaporator is 4 pass using a 'water box' arrangement at the ends of the heat exchanger. Special profiled tubes are used in evaporator to enhance the heat transfer. The details of the tube are shown in **Figure 4**.

A precise electrical thyristor controller is installed to supply the chilled water to evaporator at constant inlet temperature. This thyristor maintains the temperature fluctuations at inlet of coolant water to less than ±0.15 K. The chilled water supply is regulated at 48 l/min. Since experiments are conducted at different salt concentrations, and constant salt concentration

http://dx.doi.org/10.5772/intechopen.69299

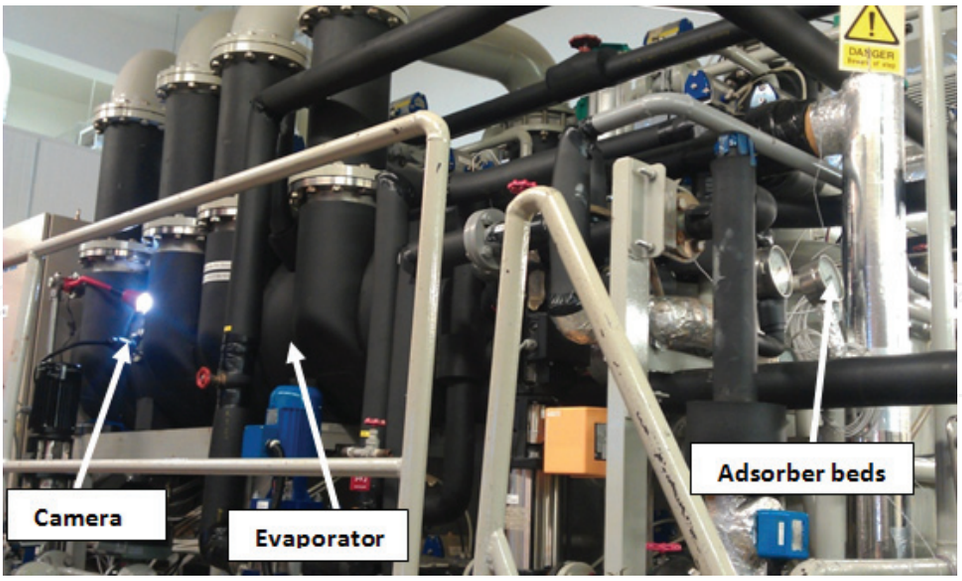

Figure 1. Pictorial view of adsorption desalination plant installed in NUS.

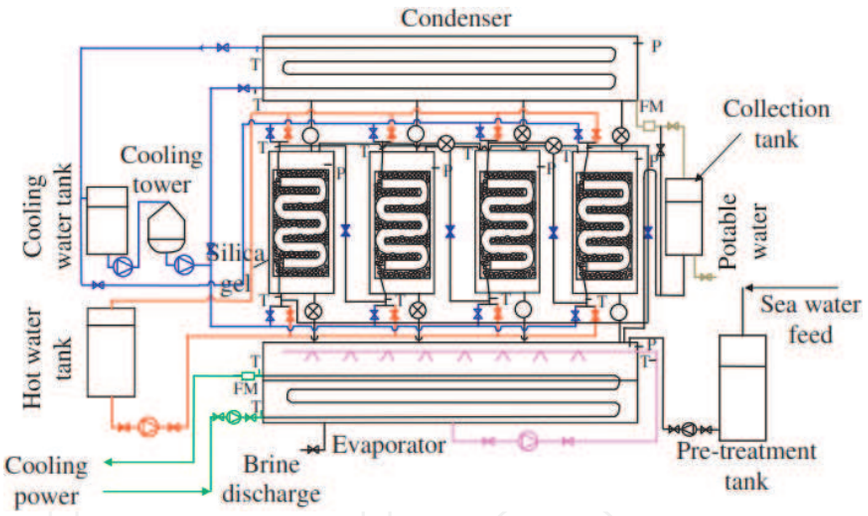

Figure 2. Detailed operational schematic of adsorption desalination plant schematic.

condition in evaporator is maintained by re-circulation of the condensate back to evaporator via U-tube. To maintain a constant liquid film on tube surface, a spray pump is used to discharge fine water droplets (nominally 0.1–0.15 mm diameter) through nozzles on top of tube bundle. The design parameters of evaporator are given in **Table 2**.

4.2.1. Experimental procedure

Experimental procedure can be categorized into operation of individual components namely: (1) evaporator, (2) Vacuum system, (3) adsorber/desorber and (4) condenser.

The evaporator operation can be divided into two circuits namely: (1) feed water circuit and (2) chilled water circuit.

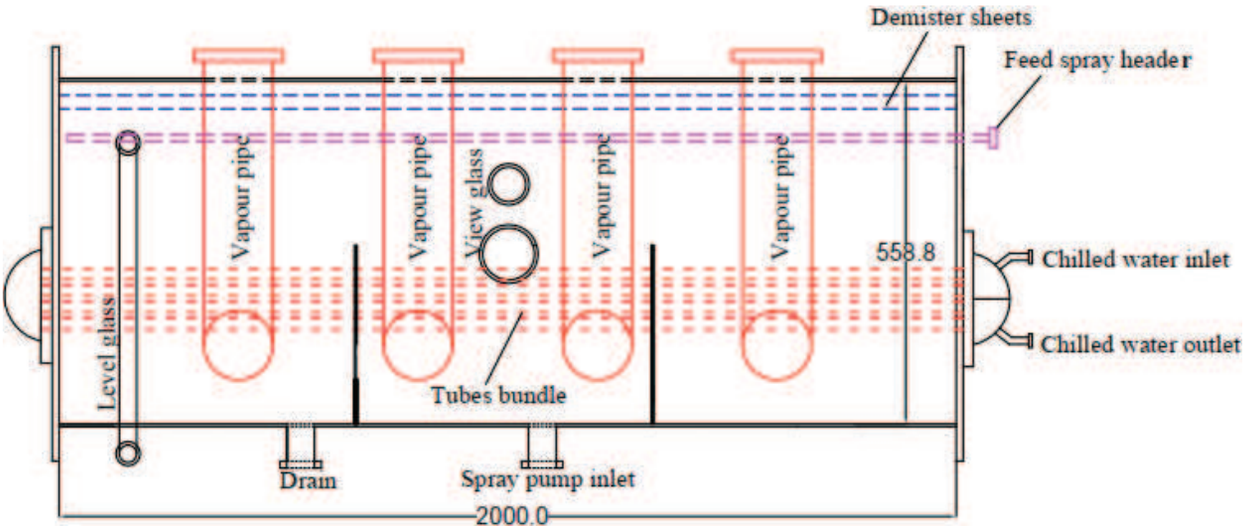

Figure 3. Adsorption desalination cycle evaporator detailed design.

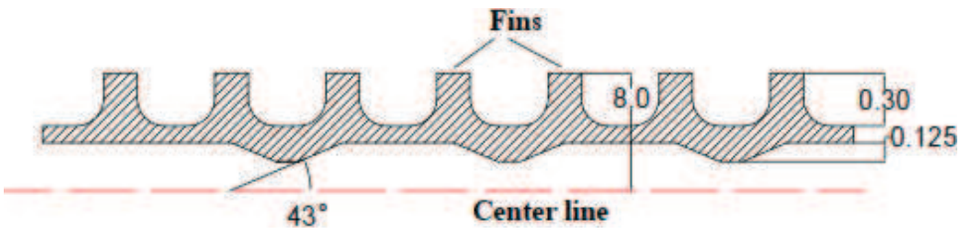

Figure 4. Cross section of end-cross tube used in evaporator of adsorption desalination plant.

Parameters	Values	Units
Number of tubes	48	
Length of each tube	1900	mm
Tube outer diameter	16	mm
Tube thickness	0.7	mm
No of passes	4	
Shell diameter	558.8	mm
Shell length	2000	mm

Table 2. Design parameters of adsorption desalination system evaporator.

4.2.1.1. Feed water circuit

The seawater/feed first enters into a pre-treatment facility to remove particulates and suspensions and then to the de-aeration tank to de-aerate. In the de-aeration tank, the dissolved non-condensable is removed before the feed enters to AD evaporator. The de-aerated feed is then pumped into the evaporator via feed pump. A spray pump is installed with evaporator to spray the feed on to the tube bundle via spray nozzles. This is special magnetic pump that can operate in vacuum environment. The reflux from condenser maintains the salt concentration

level inside the evaporator. This feed water line is provided with flow meter and valve to regulate the feed flow.

4.2.1.2. Chilled water circuit

The chilled water is the heat source that is circulated inside the tubes of evaporator. An electrical heater is installed to maintain the coolant temperature. This heater is controlled by a thyristor controller to maintain its inlet temperature. Chilled water circuit is equipped with regulating valve and flow meter to adjust the flow rate such that the evaporator can be operated under different conditions. The operation parameters are given in **Table 3**.

4.2.1.3. Vacuum system

A water vapour tolerant vacuum pump is necessary since the operation of AD system is under vacuum. Prior running an experiment vacuum holding capacity of the system is tested for 36 h, and it is found that the vacuum leak is negligible. During an experiment vacuum pump helps to maintain the desired saturation pressure inside the evaporator by pulling the air in case it ingress into the system. To ensure that the film on the tube surface is evaporating all the time, it is imminent to maintain the saturation temperature which is always lower than chilled water temperature inside the tubes.

4.2.1.4. Adsorber/desorber bed operation

The evaporator is connected to adsorber bed filled with silica gel via pneumatic valves to adsorb the water vapour. The adsorption of water vapour sustains the continuous evaporation in the evaporator. The heat of adsorption is removed by circulation of cooling water inside the adsorber coolant flow channel.

Similarly, a desorber bed is connected to a condenser and heat of desorption is supplied by a heater controlled by a thyristor controller.

4.2.1.5. Condenser operation

The desorber bed is connected to a condenser where the desorbed vapours are condensed on shell side. The cooling water circulated through the tubes of condenser is regenerated in a cooling tower at roof top.

Parameters	Values	Units
Chilled water flow rate	48	LPM
Sea water flow rate (Γ)	1.1	LPM/m of tube length
Evaporator saturation temperature	279–300	K
Evaporator saturation pressure	0.93–3.60	kPa
Feed water salinity range	15,000–90,000	ppm

Table 3. Operational parameters of adsorption desalination cycle.

The apparatus is fully instrumented to capture all required data. A Yokogawa pressure transmitter of range 0–60 KPa abs. (accuracy ±0.25%) is installed on the evaporator for saturation pressure readings. The OMEGA 5 kΩ type thermistors (accuracy ±0.15 K) are used for all temperature measurements. The KROHNE Flow meters (accuracy ±0.5% of reading) are used for flow measurements. All temperature, pressure and flow readings are continuously monitored by a data logger unit at intervals of 1 min.

A high speed camera is installed on the evaporator to observe the film behaviour over the tubes. It is observed that there is ample turbulence in liquid film on the tubes due to bubble formation on tube surface. The evidence of film turbulence is captured by camera shown in **Figure 5**, and more clear explanation by a film model is also presented.

There is a natural temperature gradient within liquid film on the tubes and the micro-bubble generation on tube surface agitates the liquid film when it tries to break through the thermal barrier. The micro-bubble generation and agitation phenomenon is explained in **Figure 6**. This

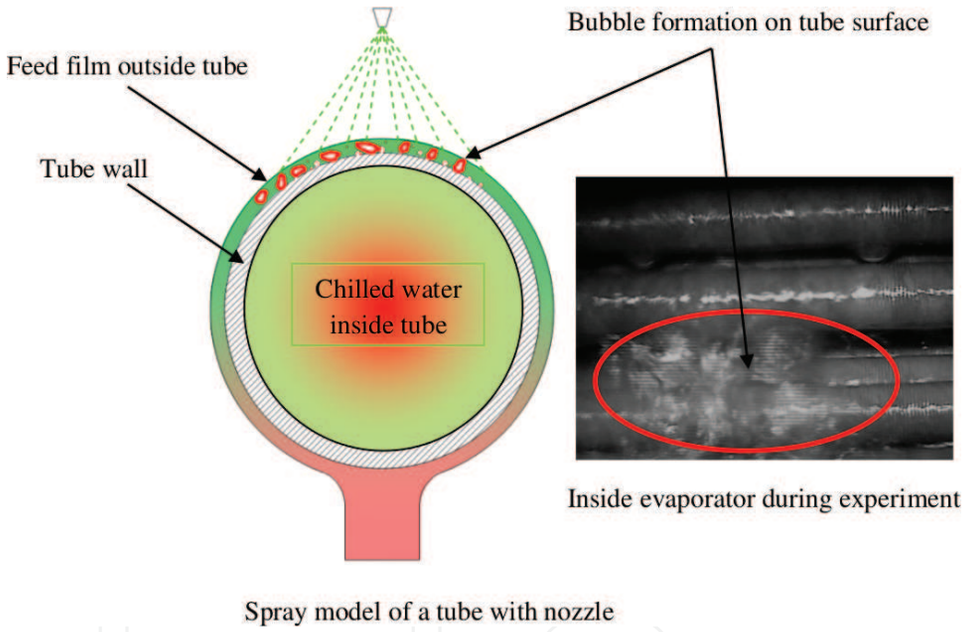

Figure 5. Bubbles formation in liquid film on tube surfaces and film agitation effect captured by camera.

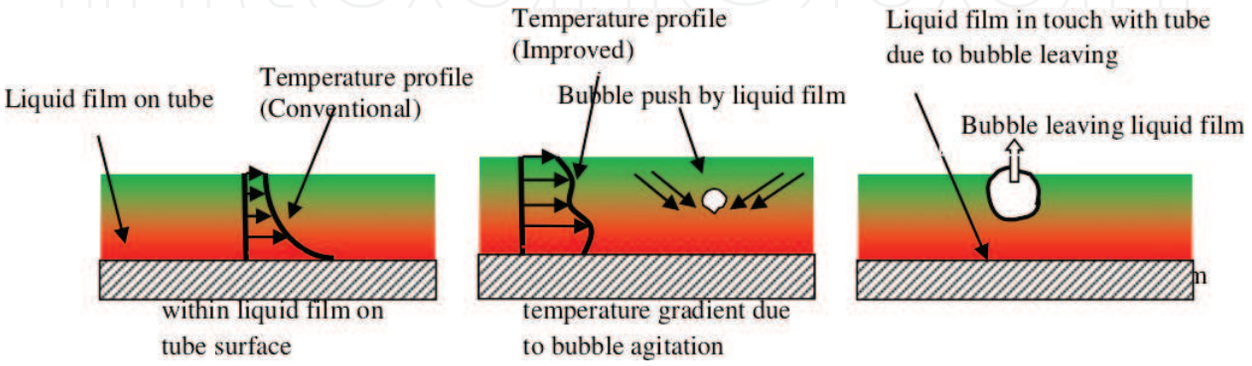

Figure 6. Film agitations due to bubbles movement and effect on conventional thermal gradient.

http://dx.doi.org/10.5772/intechopen.69299

bubble agitation has two useful effects: first, it breaks the thermal barrier between the liquid film and tube surface that enhances the local heat transfer coefficient and second, when a micro-bubble moves up to the tube surface due to its very high specific volume, it also draw the heat from tube surface which further helps to enhance the heat transfer. An additional benefit is agitation within the liquid film due to the bubble movement.

5. Results and discussion

Figure 7 shows the experimental overall heat transfer coefficient values. The heat source temperatures vary from 10 to 40°C and salt concentration is 45,000 ppm. It can be seen from the results that overall heat transfer first drop with increase in chilled water temperature and then increase again at 40°C. A similar overall heat transfer trend is observed for 60,000 ppm (60 ppt) salt concentration as shown in **Figure 8**.

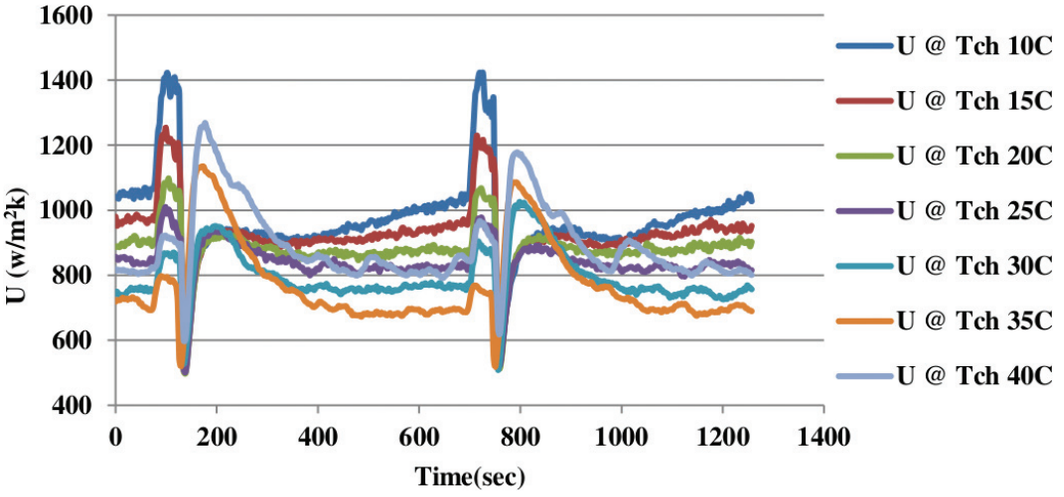

Figure 7. Typical experimental overall heat transfer coefficient profiles at 45000 ppm salt concentration.

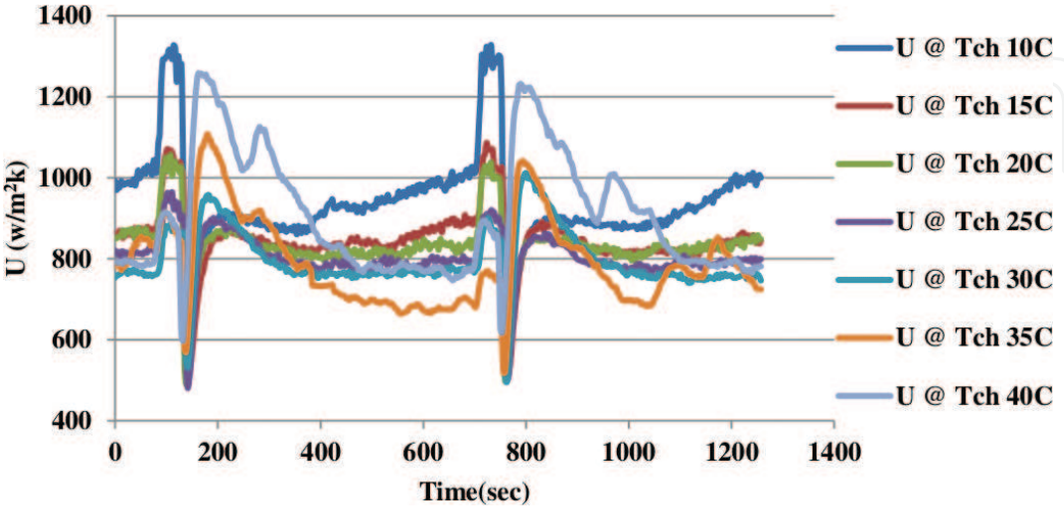

Figure 8. Typical experimental overall heat transfer coefficient profiles at 60000 ppm salt concentration.

The saturation temperature of evaporator and overall heat transfer coefficient values from experimental data at different chilled water inlet temperature and at different salt concentration are tabulated as shown in **Table 4**.

The evaporative heat transfer coefficient is calculated from experimental overall heat transfer coefficient by formulation as explained in theoretical model section. **Figure 9** shows the three-dimensional plot of evaporative heat transfer coefficients for assorted evaporator saturation temperatures and salinity level.

It can be seen from the plot that the heat transfer coefficient varies with saturation temperature and with salt concentration. It can be observed that at any salt concentration, it approaches the minimum value at 295 K and then with further decrease in saturation temperature the evaporation heat transfer coefficient value increases very sharply. It is also observed that specific volume of vapour increases very rapidly below at 295 K and above that temperature the change in specific volume of vapour is very small as shown in **Figure 10**.

It can be concluded that the sharp increase in evaporator heat transfer coefficient below 295 K may be due to bubble agitation. The micro-bubble produced on the tube surface from within the liquid film moves up quickly due to its very high specific volume and breaks the thermal barrier due to film agitation. This unique phenomenon is called 'bubble assisted evaporation'.

In film evaporation, 'micro-bubble agitation' plays an important role to enhance the heat transfer by reducing the thermal resistance between the liquid and tube surface barrier (model is shown in **Figure 6**). The traditional falling film evaporation heat transfer coefficient

Salinity	$T_{ch,in}$	T_{evap}	U	Salinity	$T_{ch,in}$	T_{evap}	U
	C	C	W/m^{2}K		C	C	W/m^{2}K
15,000	**10**	5.9	1025.45	**60,000**	**10**	5.9	937.61
	20	13.1	953.28		**20**	13.3	833.69
	30	20.3	885.17		**30**	19.7	776.62
	40	27.3	963.33		**40**	26.2	896.47
30,000	**10**	5.9	998.31	**75,000**	**10**	5.9	848.06
	20	13.1	920.78		**20**	13.0	751.47
	30	19.7	853.40		**30**	19.6	733.78
	40	25.7	906.96		**40**	26.9	893.53
45,000	**10**	5.6	970.78	**90,000**	**10**	5.5	815.94
	20	12.9	881.81		**20**	12.9	728.17
	30	19.3	798.17		**30**	19.3	694.79
	40	25.1	895.15		**40**	27.3	898.97

Table 4. Experimental overall heat transfer coefficient values and different saturation temperatures and at different salt concentrations.

http://dx.doi.org/10.5772/intechopen.69299

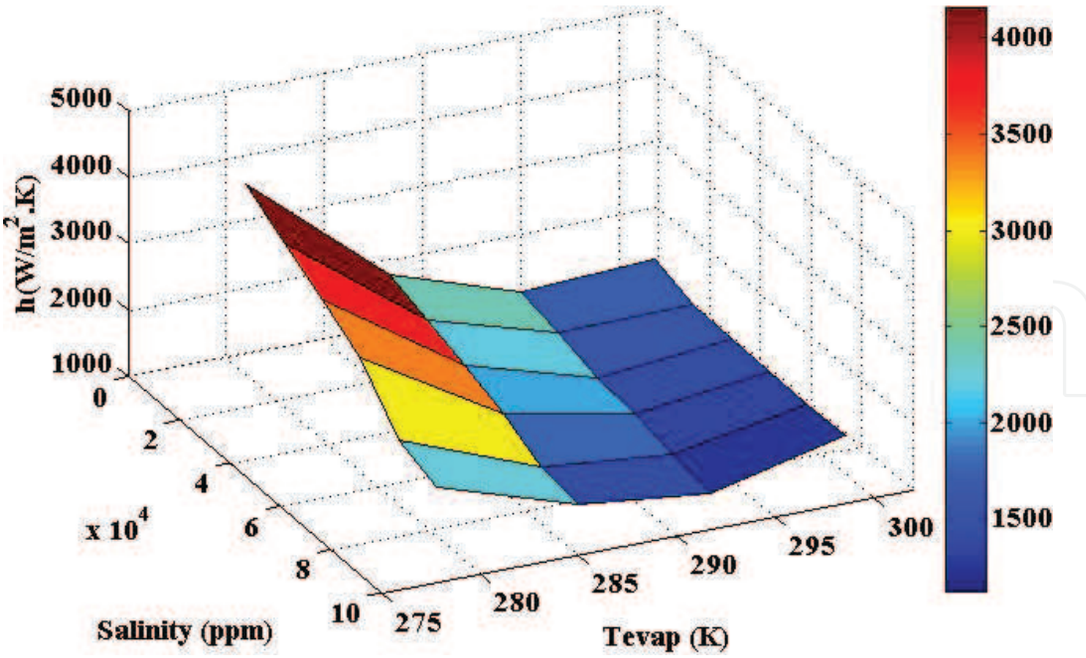

Figure 9. Experimental film evaporation heat transfer coefficient profiles at different saturation temperature and different salt concentrations.

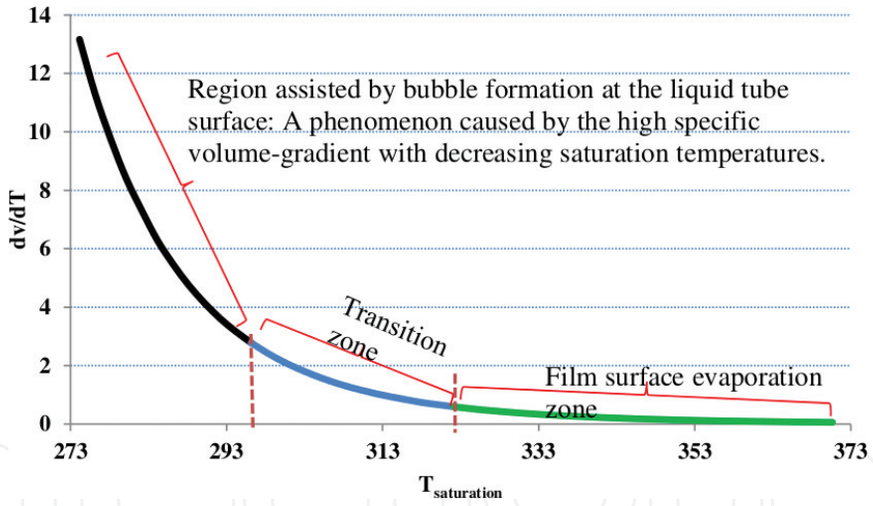

Figure 10. Change in vapour-specific volume with saturation temperature.

correlations (i.e. Han and Fletcher) do not capture this unique phenomenon and only capture the thermal driven film evaporation at saturation temperatures greater than 322 K.

A new falling film heat transfer coefficient with inclusion of 'bubble-assisted evaporation' for application at low saturation temperatures is proposed based on the experimental data. The above presented models (Eqs. 1–5) were written in FORTRAN to develop new correlation. The operational parameters namely: film velocity, salt concentration and heat flux are also included as additional parameters in the new correlation. In addition, to capture the effect of vapour specific volume, the gas volume term is also incorporated. The new correlation is given in

Eq. 3.6. **Figure 11** shows a comparison of Eq. 6 against the experimental data. It can be seen that new correlation has good agreement with experimental result. The measured heat transfer coefficient from experimental data has uncertainty of less than 8%. The Root mean square (RMS) error of regressed data is 3.5%. The additional terms used in the proposed correlation permit the limits of salinity and temperature to be accounted for, and a reference temperature, T_{ref} is taken as the reference temperature to match the region of Han and Fletcher.

$$h_{evap} = \left[0.277\left[\frac{\mu_l^2}{g.\rho_l^2.k_l^3}\right]^{-0.333}(\mathrm{Re}_\Gamma)^{-2.11}(\mathrm{Pr})^{4.55}\left[2.\exp\left(\frac{S}{S_{ref}}\right)-1\right]^{-0.41}\left(\frac{T_{sat}}{T_{ref}}\right)^{14.70}\right]+ \left[0.885.\left(\frac{q}{\Delta T}\right)^{1}.\left(\frac{v_g}{v_{ref}}\right)^{-0.34}\right] \quad (6)$$

The above correlation is suitable for sub-atmospheric conditions from 0.93 to 3.60 kPa (corresponding to saturation temperatures 279–300 K) and feed water salinity ranges from 15,000 to 90,000 ppm. The film Reynolds number ranges 45< Reᴦ < 90 and Prandtl number ranges 5< Pr < 10. In proposed superposition of effects in correlation, the first term is for film surface evaporation thermally driven and the second term is due to enhancement by the bubble assisted boiling effect.

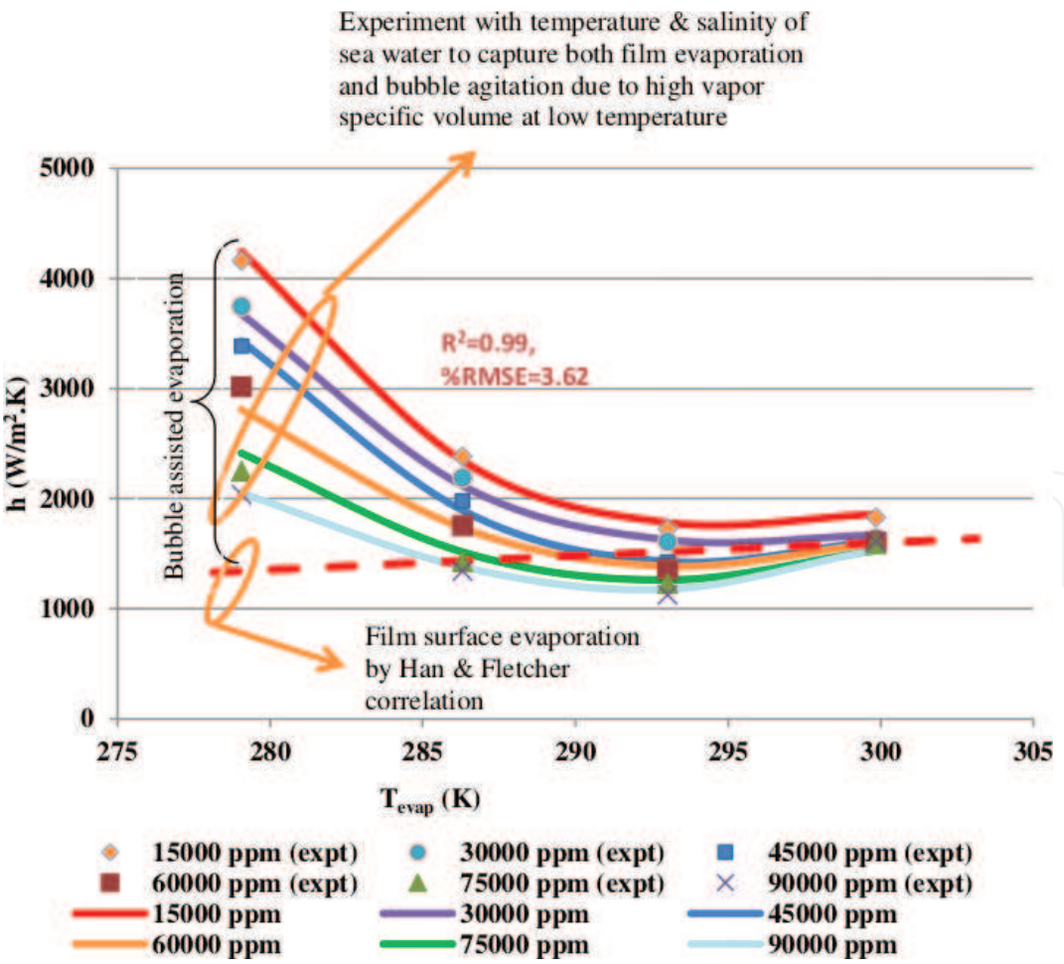

Figure 11. Falling film heat transfer coefficients values: experimental and proposed correlation.

http://dx.doi.org/10.5772/intechopen.69299

The proposed falling film heat transfer coefficient is compared with Han and Fletcher correlation extrapolated to a region outside its validation range. The Han and Fletcher correlation is for pure water. It can be seen from **Figure 12** that Han and Fletcher correlation is only suitable for thermally driven surface evaporation for saturation temperatures 322 K and above.

A unique feature of the present correlation is the capture of 'bubble-assisted evaporation' which boosts the heat transfer coefficient by two to three folds at low saturation temperature. This additional effect seems to be significant only at a low saturation temperature 295 K or below. As a consequence, for situations where cooling and desalination are required simultaneously, the design of such an evaporator is likely to be more compact than at present.

This proposed falling film heat transfer coefficient is useful for falling film evaporator design for the process industries. It also includes concentration factor to accommodate operational variables for proper heat transfer area design.

The effects of operational parameters namely: (1) salt concentration and (2) saturation temperature on heat input and LMTD are also investigated. **Figure 13** shows the effect of these parameters on heat input. It can be seen that heat input increases with saturation temperature and it is due to increase in temperature difference of heat source. It can also be observed that salt concentration effect is negligible on heat input. **Figure 14** shows the effect of saturation temperature and salt concentration on LMTD. It can be observed that LMTD also increases with saturation temperature which is due to higher temperature differences at high saturation temperatures.

The salt concentration effect is minimal as can be seen from plot. The measured accuracy of log mean temperature difference (LMTD) and the heat input (Q) is 8%.

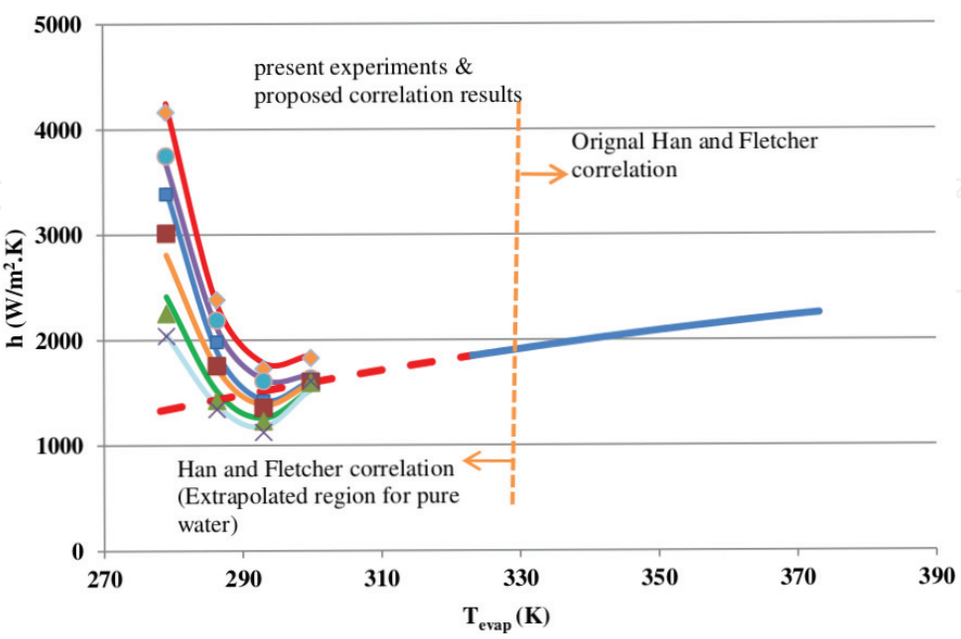

Figure 12. Falling film heat transfer coefficient values: experimental and proposed correlation compared with Han and Fletcher correlation extrapolated region.

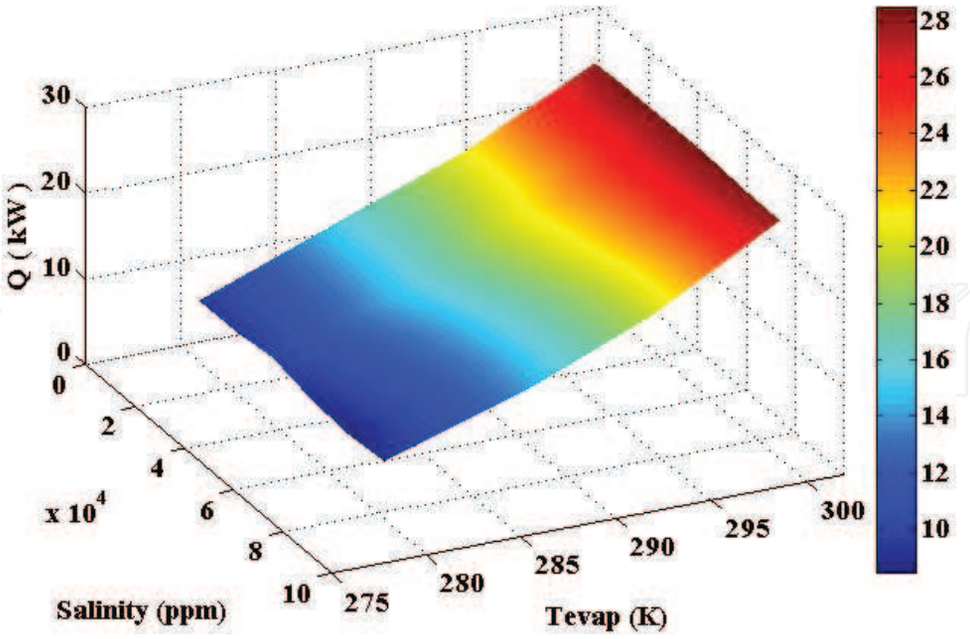

Figure 13. Effect of evaporator saturation temperature and feed salt concentration on heat input to evaporator.

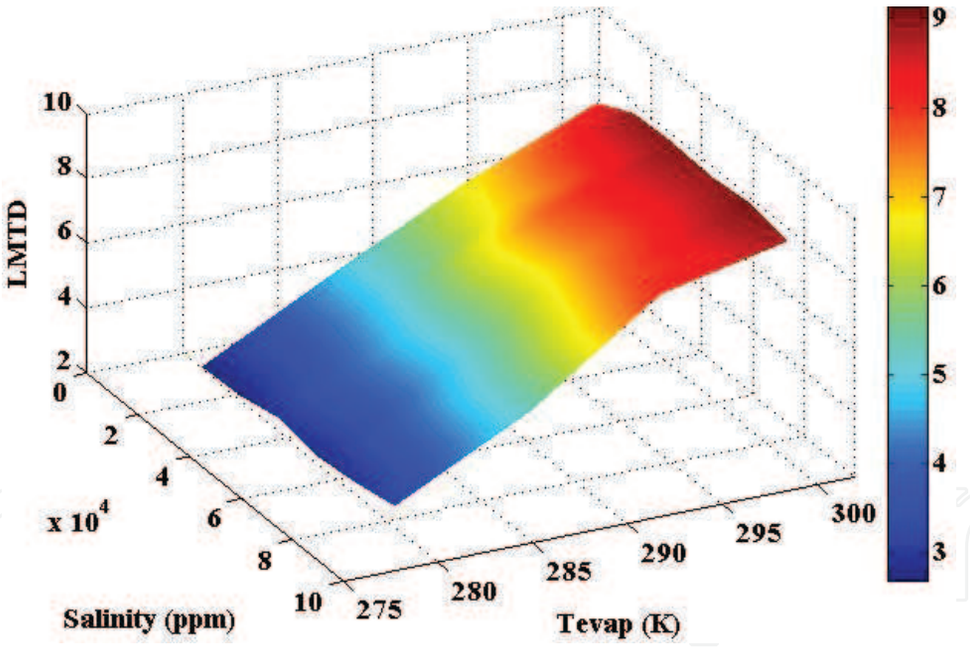

Figure 14. Effect of evaporator saturation temperature and feed salt concentration on LMTD.

6. Summary of chapter

Horizontal tube falling film evaporators can replace flooded and vertical tube evaporators because of their inherent advantages. Although horizontal falling film evaporators are advantageous, there is a lack of research data related to the heat transfer coefficient especially at low

saturation temperatures less than 323 K. The heat transfer coefficient for low saturation temperature (typically in the zone of below ambient) and for a horizontal tube evaporator of special interest to desalination applications is essential.

Experiments are conducted to investigate the heat transfer coefficient for low saturation temperatures of 279–300 K corresponding to pressure ranges of 0.93–3.60 kPa. Salt concentration in the evaporator is investigated in the range of 15,000–90,000 ppm. The heat transfer coefficient calculated from experimental data is plotted for different salt concentrations.

At low saturation temperatures, below 298 K, the tendency for liquid film to flash into vapour is made easier by the rapid increase in the specific volume of vapour. For a given thermal gradient across the liquid film, the micro-bubble is readily generated at suitable nucleation sites, such as the grooved surfaces on the tubes. This conjecture of 'bubble-agitation boiling' is backed up by photographic evidence which indicates the presence of micro-bubble generation beneath the liquid layer. The effect of micro-bubble during film boiling reduces the thermal barrier within liquid film which is responsible for enhancement of heat transfer. At low saturation temperature, the evaporation is done by two mechanisms namely: thermally driven evaporation and bubble agitation-assisted evaporation. The basic domain of validation of traditional Han and Fletcher correlation is now extended through to capture the bubble-assisted evaporation. There is heat transfer enhancement due to bubble-assisted evaporation that increases the heat transfer coefficient value from two- to four-fold

A new falling film evaporation heat transfer coefficient is proposed with parameter regression including two basic mechanisms observed during experiments. The measured heat transfer coefficient from experimental data has uncertainty of less than 8%. The RMS error of regressed data is 3.5%. The effects of operational parameters namely salt concentration and saturation temperature on heat input and LMTD are also investigated. The proposed correlation can be used for the designing of low-pressure horizontal tubes falling film evaporators for process industry.

Nomenclature

μ_1 = Liquid viscosity (kg/m-sec)

ρ_l = Liquid density (kg/m^3)

k_1= Liquid conductivity (W/m K)

Re_Γ = Film Reynolds number

Pr = Prandtl number

S = Feed water salinity (ppm)

S_o= Reference sea water salinity (30,000 ppm)

q = input heat flux (W/m^2)

T_{evap} = Evaporator saturation temperature (K)

$T_{saturation}$ = Evaporator saturation temperature (K)

T_{ref}= Reference saturation temperature (K) (T_{ref} = 322.15 K)

$T_{ch,in}$ = Chilled water inlet temperature (K)

v_g = vapour specific volume (m^3/kg)

(v_{ref} = 52. 65 m^3/kg at 295 K)

$\Delta T = T_{ch,in} - T_{evap}$

Abbreviations

EHTC	Evaporation heat transfer coefficient
FFEHTC	Falling film evaporation heat transfer coefficient
MED	Multi-effect desalination
MSF	Multi-stage flash evaporation
AD	Adsorption desalination
LMTD	Log mean temperature difference
Ppm	Part per million

Author details

Muhammad Wakil Shahzad*, Muhammad Burhan and Kim Choon Ng

*Address all correspondence to: muhammad.shahzad@kaust.edu.sa

Water Desalination and Reuse Center (WDRC), King Abdullah University of Science and Technology, Thuwal, Saudi Arabia

References

[1] Han JC, Fletcher LS. Falling film evaporation and boiling in circumferential and axial grooves on horizontal tubes. Industrial and Engineering Chemistry Process Design and Development. 1985;**24**(3):570-575

[2] Ribatski G, Jacobi AM. Falling film evaporation on horizontal tubes-a critical review. International Journal of Refrigeration. 2005;**28**(5):635-653

[3] Adib TA, Heyd B, Vasseur J. Experimental results and modeling of boiling heat transfer coefficients in falling film evaporator usable for evaporator design. Chemical Engineering and Processing. 2009;**48**(5):961-968

[4] Chun KR, Seban RA. Heat transfer to evaporating liquid films. Transactions of the ASME: Journal of Heat Transfer. 1971;**93C**(4):391-396

[5] Prost JS, Gonzaalez MT, Urbicain MJ. Determination and correlation of heat transfer coefficients in a falling film evaporator. Journal of Food Engineering. 2006;**73**(4):320-326

[6] Ahmed SY, Kaparthi R. Heat transfer studies of falling film heat exchangers. Indian Journal of Technology. 1963;**1**:377-381

[7] McAdams WH, Drew TB, Bays GS. Heat transfer to falling—water films. Transactions of ASME. 1940;**62**:627

[8] Herbert LS, Stern UJ. An experimental investigation of heat transfer to water in film flow. Canadian Journal of Chemical Engineering. 1968;**46**:401-407

[9] Uche J, Artal J, Serra L. Comparison of heat transfer coefficient correlations for thermal desalination units. Desalination. 2002;**152**(1-3):195-200

[10] Parken WH, Fletcher LS. An Experimental and Analytical Investigation of Heat Transfer to Thin Water Films on Horizontal Tubes. University of Virginia, Report UVA-526078-MAE, 1977, pp. 77-101

[11] Barba D, Felice RD. Heat transfer in turbulent flow on a horizontal tube falling film evaporator—a theoretical approach. Desalination. 1984;**51**:325-333

[12] Shah MM., A general correlation for heat transfer during film condensation inside pipes. International Journal of Heat and Mass Transfer. 1979;**22**:547-556

[13] Kutateladze SS. Fundamentals of Heat Transfer. New York: Academic Press; 1963

[14] Labuntsov DA. Heat transfer in film condensation of pure steam on vertical surfaces and horizontal tubes. Teploenergetika. 1957;**4**(7):72-79

[15] Fujita Y, Tsutsui M. Experimental investigation of falling film evaporation on horizontal tubes. Heat Transfer-Japanese Research. 1998;**27**:609-618

[16] Fujita Y, Tsutsui M, Zhou Z-Z. Evaporation heat transfer of falling films on horizontal tube - part 1, analytical study. Heat Transfer-Japanese Research. 1995;**24**:1-16

[17] Fujita Y, Tsutsui M, Zhou Z-Z. Evaporation heat transfer of falling films on horizontal tube - part 2, experimental stud. Heat Transfer-Japanese Research. 1995;**24**:17-31

[18] Liu ZH, Yi J. Falling film evaporation heat transfer of water/salt mixtures from roll-worked enhanced tubes and tube bundle. Applied Thermal Engineering. 2002;**22**(1):83-95

[19] Yang LP, Shen SQ. Experimental study of falling film evaporation heat transfer outside horizontal tubes. In: Conference on Desalination and the Environment Halkidiki, Greece; April 22-25, 2007. Desalination. 2008;**220**(1-3):654-660

[20] Parken WH, et al. Heat-transfer through falling film evaporation and boiling on horizontal tubes. Journal of Heat Transfer – Transactions of ASME. 1990;**112**(3)744-750

[21] Ribatski G, Thome JR. Experimental study on the onset of local dryout in an evaporating falling film on horizontal plain tubes. Experimental Thermal and Fluid Science. 2007;**31**(6):483-493

[22] Lorenz JJ, Yung D. Film breakdown and bundle-depth effects in horizontal tube, falling-film evaporators. Journal of Heat Transfer – Transactions of ASME. 1982;**104**(3):569-571

[23] Roques JF, Thome JR. Falling films on arrays of horizontal tubes with R-134a. Part II: Flow visualization, onset of dry out, and heat transfer predictions. Heat Transfer Engineering. 2007;**28**(5):415-434

[24] Aly G, Al-Hadda A, Abdel-Jawad M. Parametric study on falling film seawater desalination. Desalination. 1897;**65**:43-55

[25] Moeykens S, Pate MB. Spray evaporation heat transfer performance of R134a on plain tubes. Ashrae Transactions. 1994;**100**(2):173-184

[26] Moeykens S, Kelly JE, Pate MB. Spray evaporation heat transfer performance of R-123 in tube bundles. Ashrae Transactions. 1996;**102**(2):259-272

[27] Chang TB, Chiou JS. Spray evaporation heat transfer of R-141b on a horizontal tube bundle. International Journal of Heat and Mass Transfer. 1998;**42**:1467-1478

[28] Moeykens S, Pate MB. The effects of nozzle height and orifice size on spray evaporation heat transfer performance for a low-finned, triangular-pitch tube bundles with R-134a. Ashrae Transactions 1995;**101**(2):420-433

[29] Moeykens S, Pate MB. Effect of lubricant on spray evaporation heat transfer performance of R-134a and R-22 in tube bundles. Ashrae Transactions. 1996;**102**(1):410-426

[30] Moeykens S, Newton BJ, Pate MB. Effects of surface enhancement, film-feed supply rate, and bundle geometry on spray evaporation heat transfer performance. Ashrae Transactions. 1995;**101**(2):408-419

[31] Bourouni K, Martin R, Tadrist L, Tadrist H. Modelling of heat and mass Transfer in a horizontal tube falling film evaporators for water desalination. Desalination. 1998;**116**: 165-184

[32] Yang L, Shen S. Experimental Study of Falling Film Evaporation Heat Transfer outside Horizontal Tube. Desalination. 2008;**220**:654-660

[33] Xu L, Ge M, Wang S,Wang Y. Heat Transfer Film Coefficients of Falling Film Horizontal Tube Evaporators. Desalination. 2004;**166**:223-230

[34] Yang L, Shen S. Experimental study of falling film evaporation heat transfer outside horizontal tubes. Desalination. 2008;**220**:654-660

[35] Chun KR, Seban RA. Heat Transfer to evaporating liquid films. ASME Journal of Heat Transfer. 1971;**11**:391-396

[36] Alhusseini AA, Tuzla K, Chen JC. Falling film evaporation of single component liquids. International Journal of Heat and Mass Transfer. 1998;**41**(12):1623-1632

[37] Shmerler JA, Mudawwar I. Local evaporative heat transfer coefficient in turbulent free-falling liquid films. International Journal of Heat and Mass Transfer. 1988;**31**(4):731-742

[38] Chien LH, Tsai YL. An experimental study of pool boiling and falling film evaporation on horizontal tubes in R-245fa. Applied Thermal Engineering. 2011;**31**:4044-4054